EXPERIMENT NO. M-557

IMMISCIBLE ALLOY COMPOSITIONS

By

J. L. Reger
TRW Systems Group
Redondo Beach, California 90278

SUMMARY

Ampoules containing materials exhibiting either liquid or solid state immiscibility were thermally processed in the M-518 Multipurpose Electric Furnace under low and one gravity conditions. Three cartridges, each containing three separate experiment ampoules were processed simultaneously during one furnace run.

Two of the experiment ampoules, gold-germanium (Ampoule A) and lead-zinc-antimony (Ampoule B), were processed in the isothermal portion of the furnace and one experimental ampoule, lead-tin-indium (Ampoule C), was processed in the gradient region of the furnace. Both the control (one gravity) and low gravity processed specimens were analyzed for their metallographic and electronic properties.

In all cases, the low gravity processed specimens exhibited better homogenization and microstructural appearances than the one gravity control specimens. The electronic behavior of the low gravity specimens were equal or superior in every respect and the Ampoule B specimens exhibited an anomalous superconducting transition temperature approximately 2 K higher than either the elements or the one gravity control specimens. In addition, the low gravity processed A and B ampoules exhibited X-ray diffraction lines not identifiable with any referenced diffraction patterns.

From these analyses, it is concluded that low gravity processing of materials processing liquid or solid immiscibility can produce compositions exhibiting unusual metallographic and electronic behavior.

INTRODUCTION

Immiscible systems, with few exceptions, are one of the unique classes of materials which are non-producible in bulk form on Earth. A number of these systems provides a potential class of new materials if they can be successfully produced in space. These potential applications include electronic, optical and other types of materials with unique physical characteristics.

Since segregation effects due to density differences and the relatively long time period necessary to solidify the materials from

the liquid state are the primary reasons for inability to secure bulk samples, processing in a low gravity environment should circumvent the majority of the problems associated with the immiscible systems.

This hypothesis has been verified to a large degree by investigations at TRW Systems Group utilizing NASA low gravity facilities to process materials having a miscibility gap in either the liquid or solid state [References 1, 2, 3].

In one of these investigations, however, it was found that the cooling rate during low gravity solidification had an influence on both the microstructure and electrical behavior of the immiscible system [References 2,4].

Thus, the opportunity of processing systems having either liquid or solid immiscibility on Skylab should provide extremely valuable information in corroborating both current information on the behavior of these systems, as well as a comparison of the effect of long cooling times with the results obtained in the short duration, low gravity facilities.

SKYLAB TESTS

Experiment M-557: "Immiscible Alloy Compositions", is comprised of three separate specimen ampoules per cartridge processed in the M-518 Multipurpose Electric Furnace; two in the isothermal portion and one in the gradient region of the furnace. The isothermal ampoules, designated A and B, contain 76.85 - 23.15 w/o gold-germanium and 45.05 - 45.06 - 9.89 w/o lead-zinc-antimony, respectively. Ampoule A, gold-germanium, exhibits almost complete solid state immiscibility and Ampoule B, lead-zinc-antimony, exhibits a liquid miscibility gap below a critical or consolute temperature. The gradient ampoule, designated C, contains 70.20 - 14.80 - 15.00 w/o lead-tin-indium, with tin as the precipitated second phase. Figure 1 shows the cartridge and ampoule configuration.

Two sets of three cartridges each were processed under one gravity conditions as controls; three horizontally and three vertically in the furnace. Three cartridges were then subsequently processed in the M-512/M-518 facility on board Skylab during the SL-3 mission. Basically, the processing consists of heating the isothermal section of the cartridges to 720°C, holding the temperature for a soak period of 4 hours, then allowing the cartridges to passively cool to ambient temperature. This temperature was set to allow Ampoule B to be heated above the critical or consolute temperature where the liquid immiscibility gap is exceeded and the liquid elements become single phase. The soak period is sufficiently long for complete mixing and diffusion of the elements. The temperature at the cold end is clamped such that Ampoule C is not completely melted, thus a comparison of the solidification behavior between one gravity and low gravity processed specimens can be made.

A AMPOULES

Figures 2 and 3 represent photomacrographs of one and low gravity processed gold-germanium specimens. As can be seen, precipitation/segregation

of the germanium mainly occurs at the top of the one gravity specimens, as opposed to the more random distribution in the low gravity processed specimens.

Microscopic documentation was primarily limited to the low gravity specimens, since the gross segregation of the one gravity processed specimens prevented any extensive interpretation. In essence, the density differences between the elements dominated to the extent that minimal interaction in terms of microstructural differences occurred.

Figures 4 through 6 are optical, electron microprobe and scanning electron photomicrographs of typical specimen areas. For the most part, the areas are identical for each type of instrument utilized and are representative of the specimen microstructure. Some differences in microstructural appearance are evident between the surface and the interior of the specimens; however, the presence of either a very fine dispersion or a compound is still evident. In addition, comparison of gold-germanium specimens from another program [Reference 3] cooled at much faster rates with those on this program (an example is Figure 7) show that cooling time does play an important role in the microstructural features of immiscible systems.

Table I presents the X-ray diffraction data of the specimens which do not correspond to the known diffraction data of the elements and the metastable gamma germanium gold. Both unknown lines of varying intensities were found. If the lines correspond to a metastable compound, the varying intensity may be due to the orientation within the specimen since it has been noted that both the d spacing and the intensity will vary as a function of orientation [Reference 5].

Superconductivity measurements were made on the bulk specimens by the inductance method as shown schematically in Figure 8 . None of the one gravity but all of the low gravity processed specimens superconducted at 1.5 K, although the signal was weak. This indicates that only a small portion of the specimen superconducts, possibly correlating to the fine dispersions. Superconducting transition temperatures are shown in Figure 9.

Resistivity measurements using a Leeds four point probe were made on the one and low gravity processed specimens and the results are shown in Figure 10 . As can be seen, the resistivity of the one gravity processed specimens decreases toward the gold rich end due to the gravity gradient. The values are higher than for pure gold since some germanium is present.

B AMPOULES

Figures 11 and 12 are photomacrographs of the one and low gravity processed lead-zinc-antimony specimens. As with the gold-germanium, extensive segregation occurred in the one gravity specimens and microscopic documentation was primarily limited to the low gravity processed specimens since the segregation again prevented meaningful interpretation. Figures 13 through 15 are optical, electron microprobe and scanning electron photomicrographs of typical specimen areas.

The low gravity processed specimens are not only more uniformly dispersed, but additionally zinc is the primary matrix, with lead as the dispersant and antimony is predominantly associated with the zinc, as opposed to the one gravity processed specimens.

As with the A Ampoules, the X-ray diffraction patterns of the low gravity processed specimens show additional lines which do not correspond with any of the known elements or compounds. Table II presents the d spacings and intensities.

Superconductivity measurements were made on the B specimens in the same manner as with the A specimens and the results are shown in Figure 16. Both the one and low gravity specimens exhibited the same superconducting behavior to 7.2K, but the low gravity specimens had an additional transition at 9.2K, which is 2K higher than any of the three compositional elements. The reason for this anomalously high transition temperature is not known, although it may be due to the fine dispersion of lead in the zinc-antimony matrix leading to a fine particle superconductivity effect [References 6 and 7].

As with the A specimens, resistivity measurement were made with the Leeds four point resistivity probe and are shown in Figure 17. Again, a more uniform resistivity was noted with the low gravity as compared to the one gravity processed specimens.

C AMPOULES

Due to the nature of the electronic testing performed on these materials, minimal metallagraphic documentation was done on these specimens. Figures 18 and 19 exemplify the transition zone where solidification started and the directional solidification that occurred during cooldown. In general, the directional microstructure of the low gravity processed specimens is finer and of better quality than the controls. Table III gives the X-ray data for the specimens; there was no appreciable difference between the one and low gravity specimens.

Magnetic measurements were carried out on the directionally solidified Pb-Sn-In C specimens processed in one and in low-gravity environment. Dispersion of the Sn-rich phase, which is non-superconducting at 4.2 K, may act as pinning sites to flux movement [Reference 8], resulting in hysteresis effects with large areas under the magnetization curves. If Pb-rich lamellar structures of small dimensions are formed by directional solidification, this may be apparent in an increase in H_{c2}.

Both the one and low gravity processed specimens were sectioned such that the maximum and minimum G/R ratio portions as shown in Figure 20 were measured to determine the effect of directional perfection, etc. on the magnetic properties. The samples were cut in 2 cm lengths and placed to fit tightly in the center of coils wound with 10,000 turns of #36 copper magnet wire to length of 3.4 cm. Permeability measurements were made as a function of the magnetic field by measuring the inductance with a bridge at 1 kHz with the coils placed in the center

of a superconducting solenoid with the axes approximately parallel to the field. Three coils could be arranged symmetrically about the axis of the solenoid with the center of the samples separated by 2.5 cm. This allowed the samples to be within a sphere of less than 1% inhomegeneity in the magnetic field. All measurements were made with the samples immersed in liquid helium at a temperature of 4.2K. A schematic diagram of the apparatus is shown in Figure 21.

A typical magnetization curve is shown in Figure 22 and the data is presented in Table IV, where "cold end" refers to the section of sample cut from the region processed with a high G/R ratio. Hysteresis effects are apparent indicating the presence of trapped flux. This is the region where the greatest amount of two phase directional solidification is expected [References 9,10].It is noted that with the one gravity processed samples there is little correlation in H_{c2} values between the high and low G/R specimens. The low gravity processed samples, however, show consistently higher H_{c2} values for the portion having a high G/R ratio. These samples also show somewhat more pronounced hysteresis with larger areas under the curves, indicating more extensive flux pinning by the Sn-rich phase. These results correspond to a greater extent of directional solidification with low gravity processing compared to the one gravity processed samples. In the region of high G/R ratio (cold end), the low gravity processed samples show an average increase in H_{c2} of 260 Oe, compared to the one gravity processed samples.

CONCLUSION

Three systems possessing either liquid or solid state immiscibility have been processed in the M-518 facility on board Skylab. From the metallurgical and electronic examinations, the low gravity processed specimens exhibited unique metallurgical features and enhanced electronic properties as contrasted to the one gravity processed controls.

The A specimens corroborated the effect of cooling rate on the metallurgical structure.

The unknown X-ray diffraction lines exhibited by the low gravity processed A and B specimens indicates that processing in this type of environment can lead to morphological structures not found in the one gravity processed specimens. It is not known at this time if the unusual superconducting transitions found in these systems are related to these diffraction patterns.

Inasmuch as a low gravity environment suppresses thermal convection, high G/R ratios can be utilized to obtain directionally solidified structures having superior metallurgical and electronic features, exemplified by the C specimens, as contrasted to the one gravity processed specimens.

It must be emphasized that these materials represent only a

fraction of the hundreds of systems possessing a miscibility gap which have been identified. However, the interesting electronic and metallurgical behavior of these processed materials has lead to cautious optimism regarding the potential use of this class of materials. Thus from this work, it is anticipated that future research into immiscible systems will benefit not only the basic understanding of materials behavior but ultimately enable materials to be produced which will have extremely useful applications.

REFERENCES

1. "Test and Evaluation of Apollo 14 Composite Casting Demonstration Specimens 6, 9 and 12," Contract NAS 8-27085, Phase I, TRW Systems Group, Redondo Beach, CA
2. "Test and Evaluation of Apollo 14 Composite Casting Demonstration Specimens 6, 9 and 12," Contract NAS 8-27085, Phase III, TRW Systems Group, Redondo Beach, CA
3. J. L. Reger, "Study on Processing Immiscible Materials in Zero Gravity," Contract NAS 8-28267, TRW Systems Group, Redondo Beach, CA
4. L. L. Lacy and G. H. Otto, "The Electrical Properties of Zero Gravity Processed Immiscibles" Paper No. 74-208, presented at the AIAA 12th Aerospace Sciences Meeting, Jan 30 - Feb 1, 1974, Washington, D. C.
5. T. R. Anantharaman, et al, Trans. A.I.M.E., 233, 2014 (1965).
6. J. Hurault, "Superconductivity in Small Crystallites," J. Phys. Chem. Solids 29, 1765 (1968).
7. J. H. P. Watson, "Possibility of Ultrahigh Critical Fields in Granular Hard Superconductors," Appl. Phys. Letters 15, 125 (1969).
8. J. D. Livingston, "Flux Pinning by Superconducting Precipitates," Appl. Phys. Lett. 8, 319 (1966).
9. F. R. Mollard and M. C. Flemings, "Growth of Composites from the Melt-Part I ," Trans. TMS - AIME 239, 1534 (1967).
10. F. R. Mollard and M. C. Flemings, "Growth of Composites from the Melt-Part II," Trans. TMS - AIME 239, 1534 (1967).

Table I. Unknown X-Ray Diffraction Lines for A Specimens

d Spacing, Å	I/I_o [1]	Specimens [2]
1.992	8	11
1.293	10	12
1.021	2,5,3	10,11,12
0.9108	7,26,29	10,11,12
0.8926	32	12
0.8334	7,33,30	10,11,12
0.8307	11	12

Table II. Unknown X-Ray Diffraction Lines for B Specimens

d Spacing, Å	I/I_o [1]	Specimens [2]
3.450	4,12	10,12
3.437	27	11
2.976	14	11
2.3.3	15,5	10,12
2.135	15,17	6,11
2.004	22	10
1.489	49	11
1.336	10	11
1.310	11,4	11,12
1.255	38	12
1.133	25,9	11,12
1.008	7,7,10	10,11,12
0.9503	11,8,10	10,11,12
0.8656	12	12
0.8346	7,7,5	10,11,12

Table III. Unknown X-Ray Diffraction Lines for C Specimens

d Spacing, Å	I/I_o [1]	Specimens [2]
3.048	42	All
2.840	60	All

1. Ratio of line intensity to strongest peak
2. Both one and low gravity processed specimens

Note: All other lines identified.

Table IV. H_{c2} Values for Pb-Sn-In Eutectic Alloys *

Sample (1-g)	H_{c2} (kOe)	Sample (low-g)	H_{c2}(kOe)
1 C cold end	3.62	10 C cold end	3.88
1 C hot end	3.69	10 C hot end	3.80
2 C cold end	3.76	11 C cold end	4.06
2 C hot end	3.66	11 C hot end	3.60
3 C cold end	3.67	12 C cold end	3.89
3 C hot end	3.90	12 C hot end	3.62

* Average H_{c2} values for Pb-Sn-In eutectic alloys

	One-g processed	Low-g processed
Cold end	3.68 kOe	3.94 kOe
Hot end	3.75 kOe	3.67 kOe

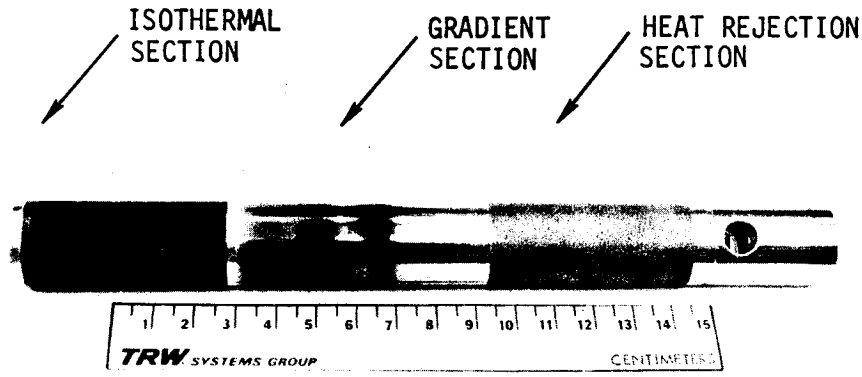

PROCESSED M-557 CARTRIDGE SHOWING EXTERNAL CONFIGURATION

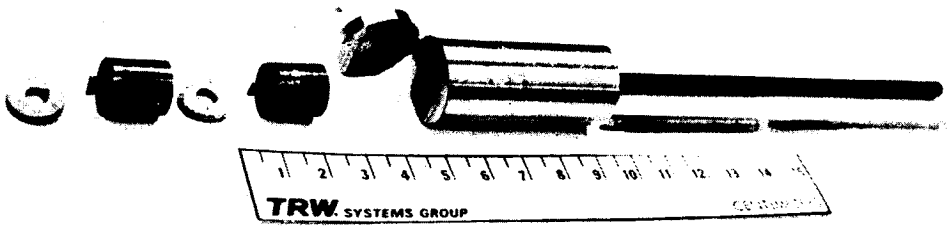

DISASSEMBLED AMPOULE SET

FIGURE 1. M-557 CARTRIDGE AND AMPOULE CONFIGURATION

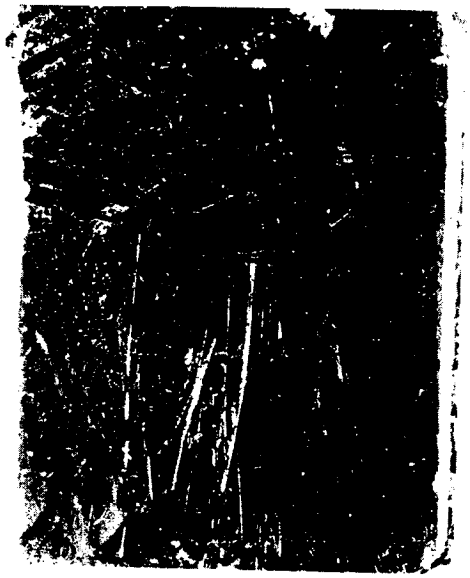

Specimen 1A

Specimen 5A

Specimen 12A

FIGURE 2. ONE GRAVITY PROCESSED SPECIMENS 1A and 5A AND LOW GRAVITY PROCESSED SPECIMEN 12A (10X)

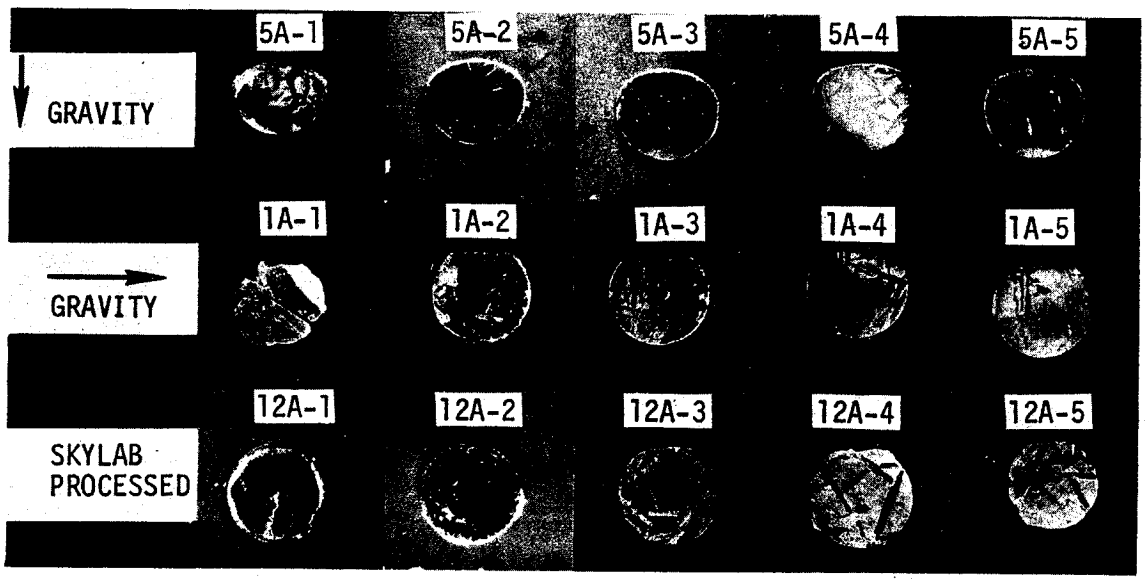

Figure 3. Axially Sectioned Specimens 1A, 5A and 12A (1.5X)

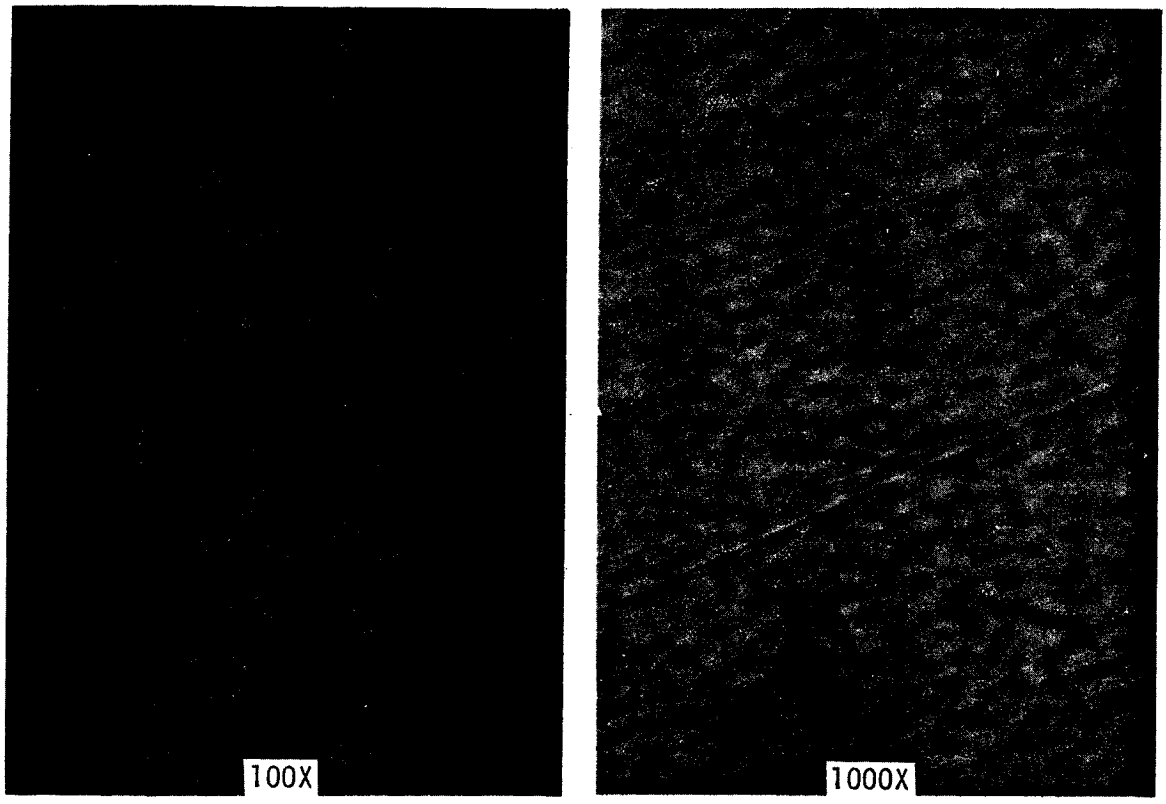

FIGURE 4. OPTICAL PHOTOMICROGRAPHS OF SECTION 12A - 2

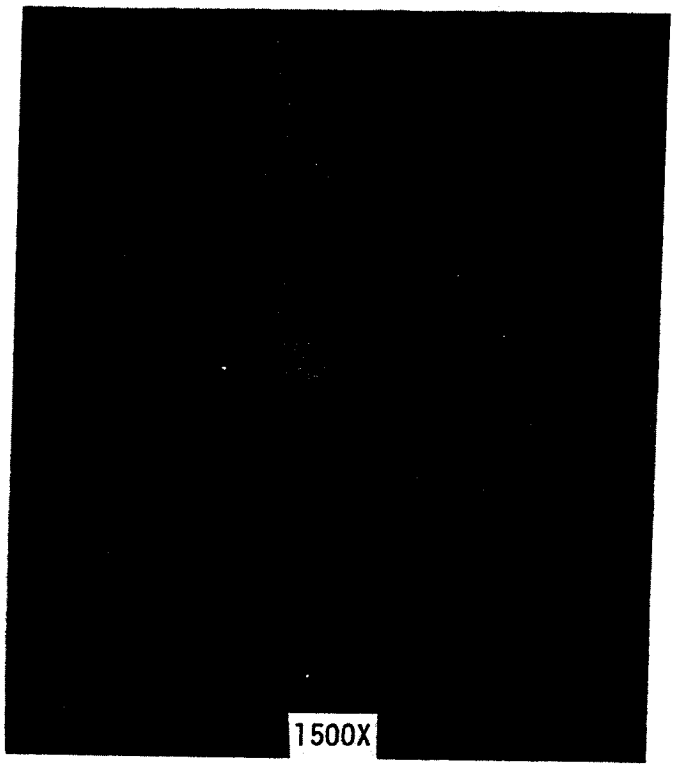

FIGURE 5. SEM PHOTOMICROGRAPHS OF SECTION 12A - 2

absorbed electron

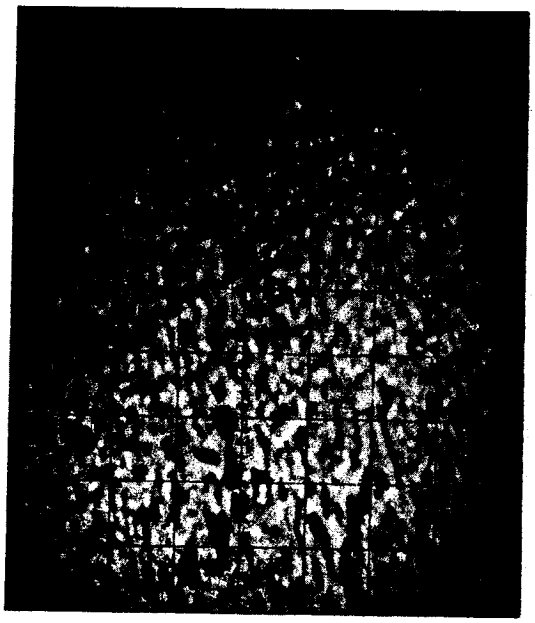

Au

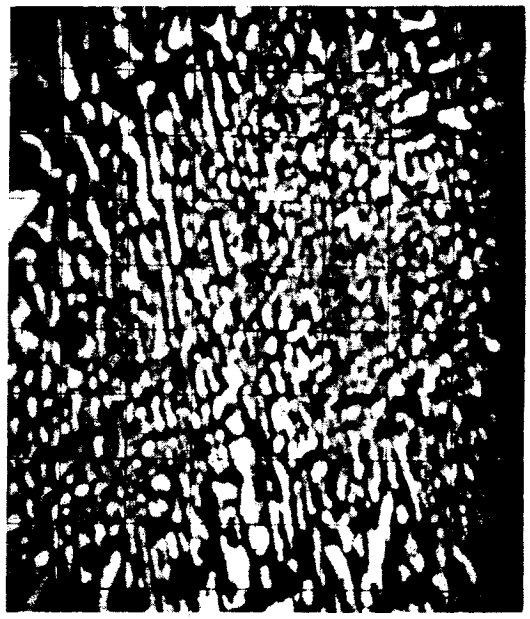

Ge

FIGURE 6. ELECTRON MICROPROBE PHOTOMICROGRAPHS
OF SECTION 12A - 2 (900X)

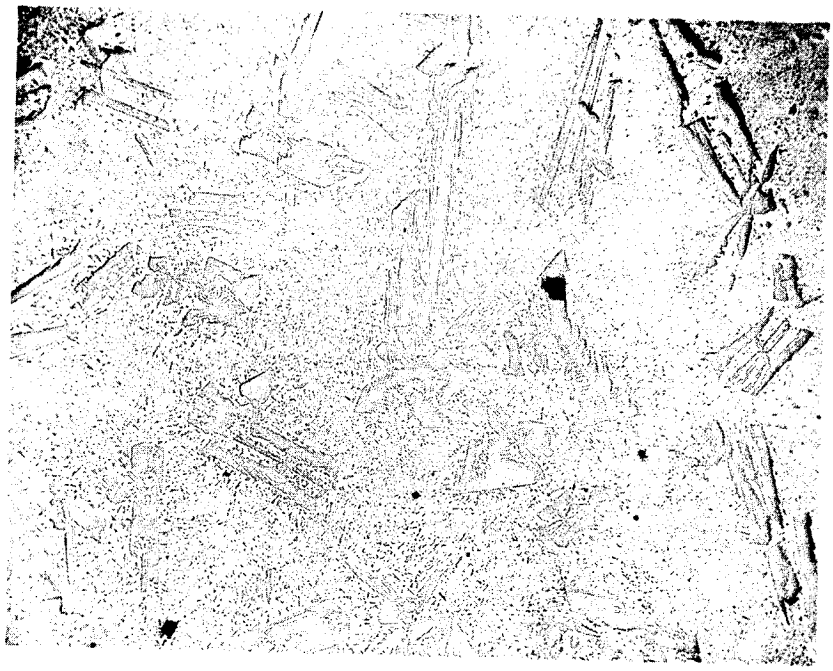

Specimen 1-C

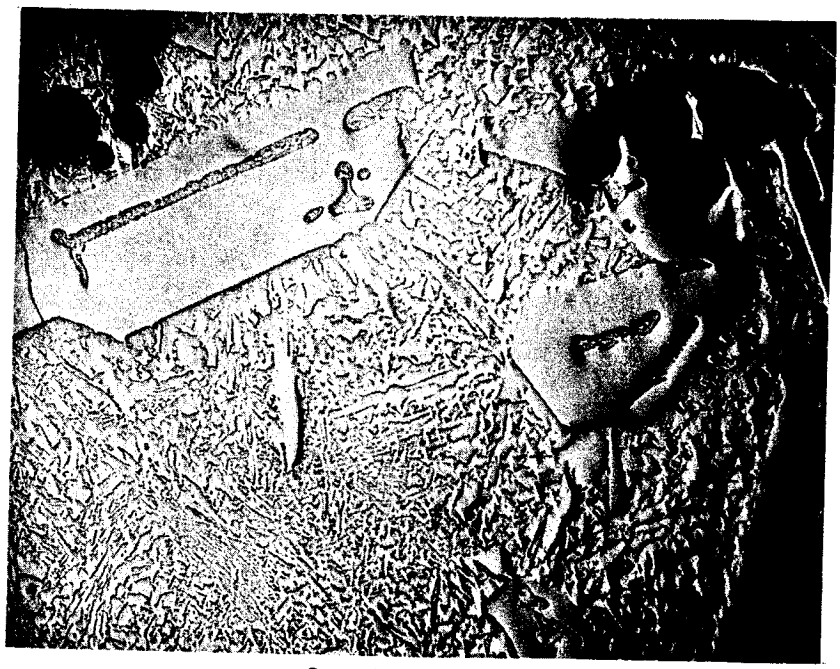

Specimen 12A

FIGURE 7. SPECIMEN 12A VERSUS KC-135 PROCESSED SPECIMEN 1-C (50X)

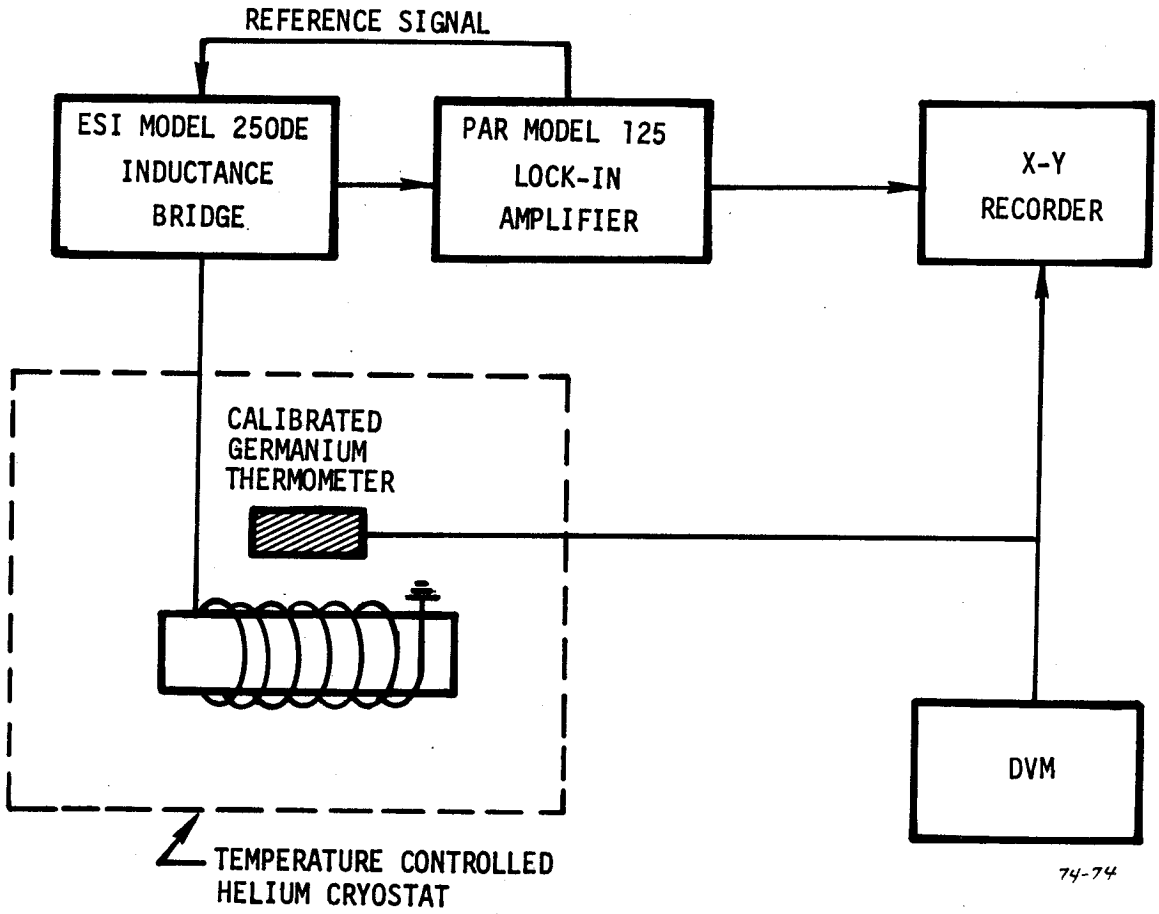

FIGURE 8. SCHEMATIC BLOCK DIAGRAM FOR INDUCTANCE MEASUREMENTS

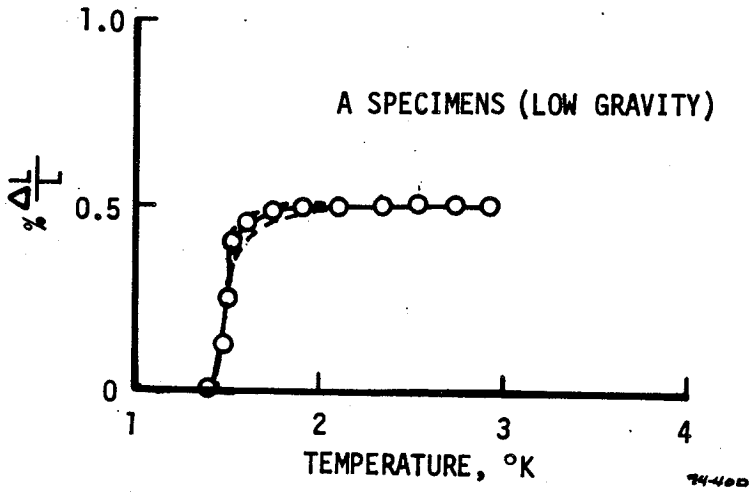

FIGURE 9. SUPERCONDUCTING TRANSITION TEMPERATURES OF A SPECIMENS

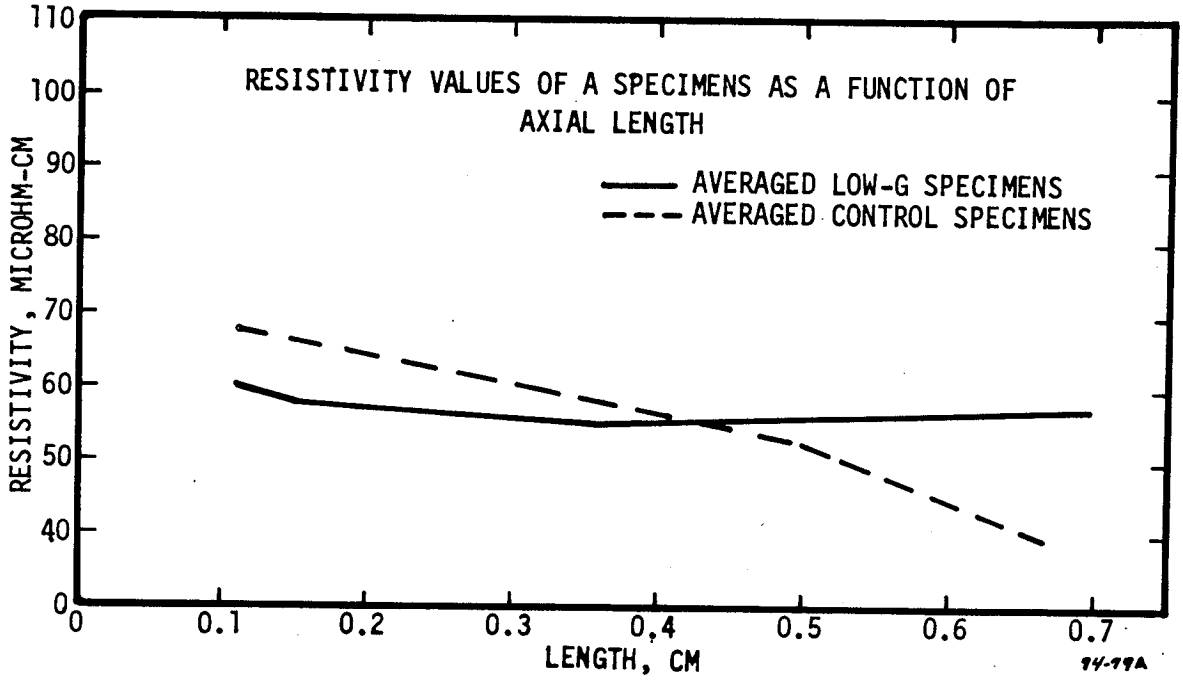

FIGURE 10. RESISTIVITY OF CONTROL AND LOW GRAVITY PROCESSED A SPECIMENS

Specimen 3B

Specimen 5B

Specimen 12B

FIGURE 11. ONE GRAVITY PROCESSED SPECIMENS 3B AND 5B AND LOW GRAVITY PROCESSED SPECIMEN 12B (10X)

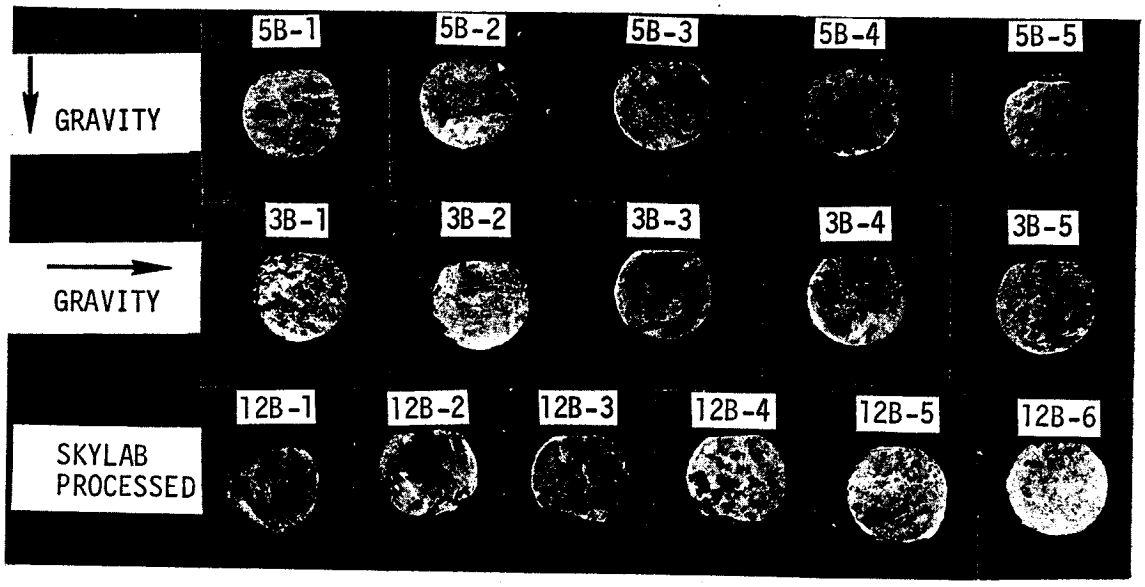

FIGURE 12. AXIALLY SECTIONED SPECIMENS 3B, 5B AND 12B (1.5X)

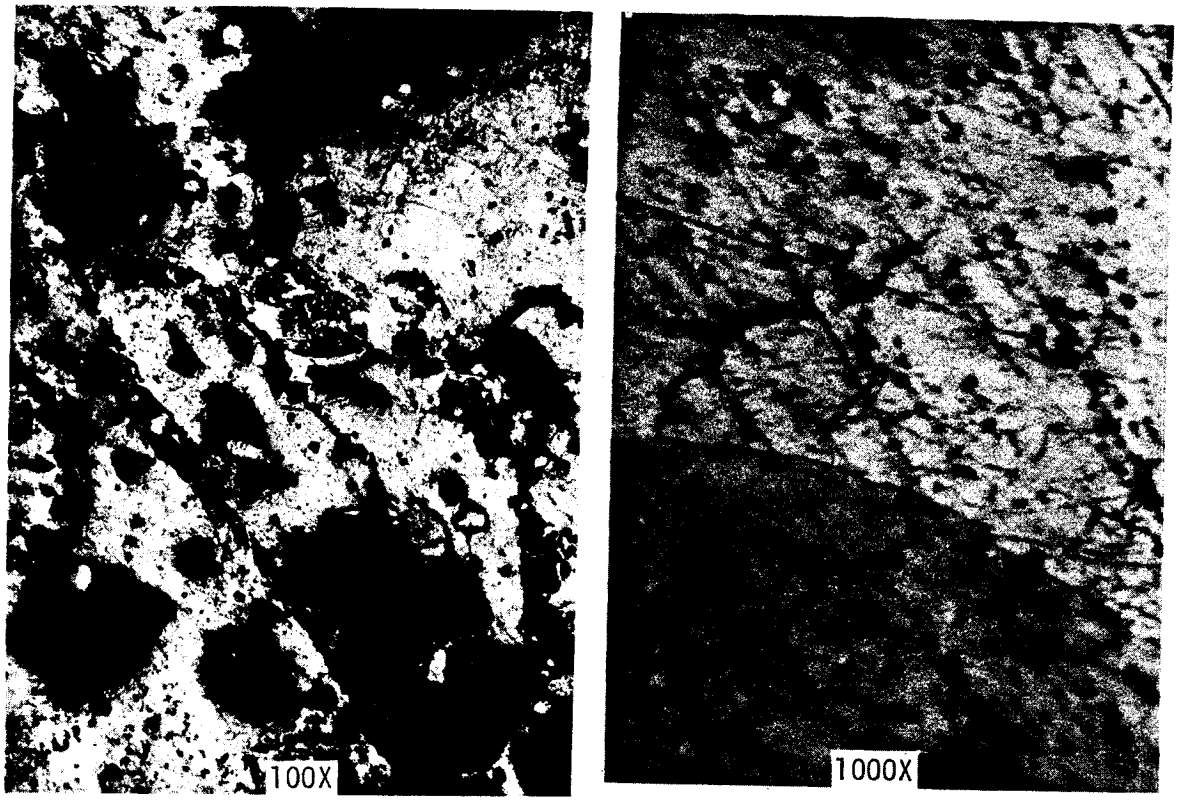

FIGURE 13. OPTICAL PHOTOMICROGRAPHS OF SECTION 12B - 2

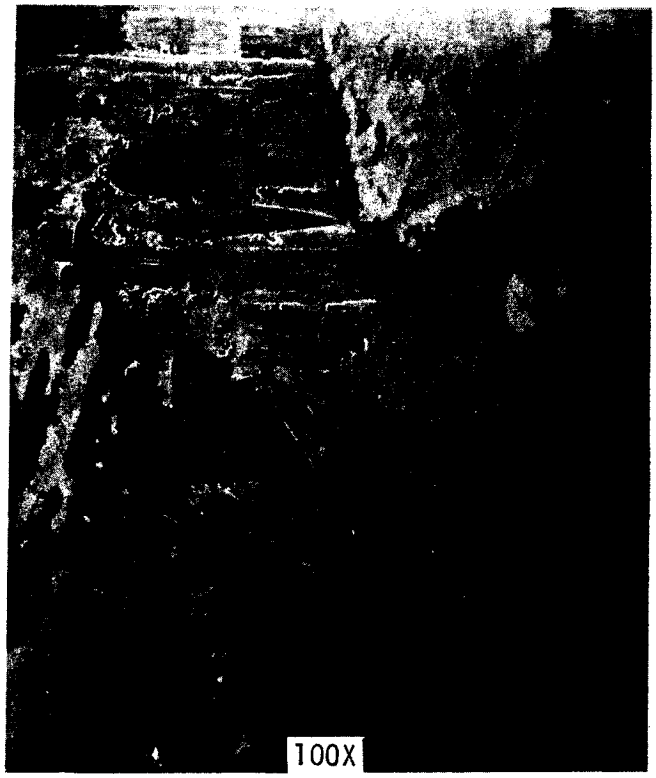

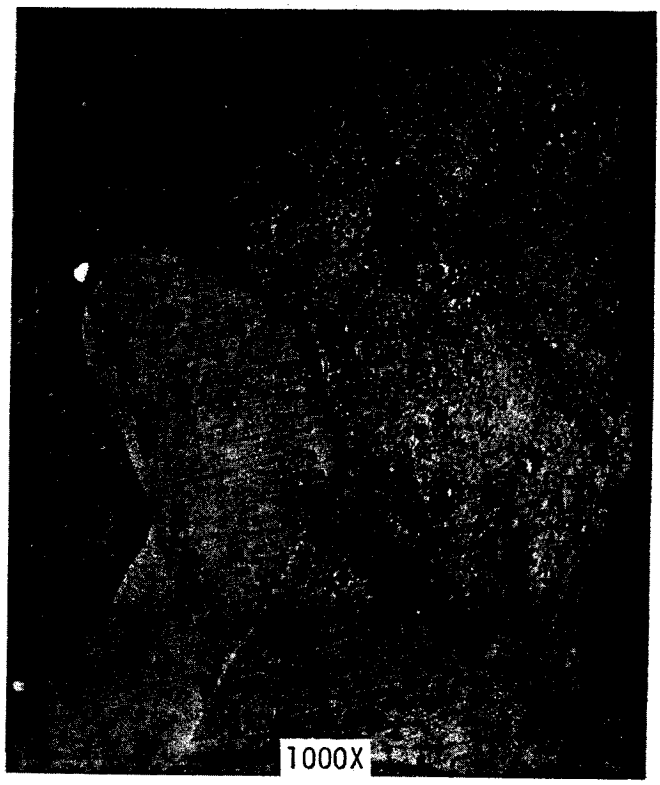

FIGURE 14. SEM PHOTOMICROGRAPHS OF SECTION 12B - 2

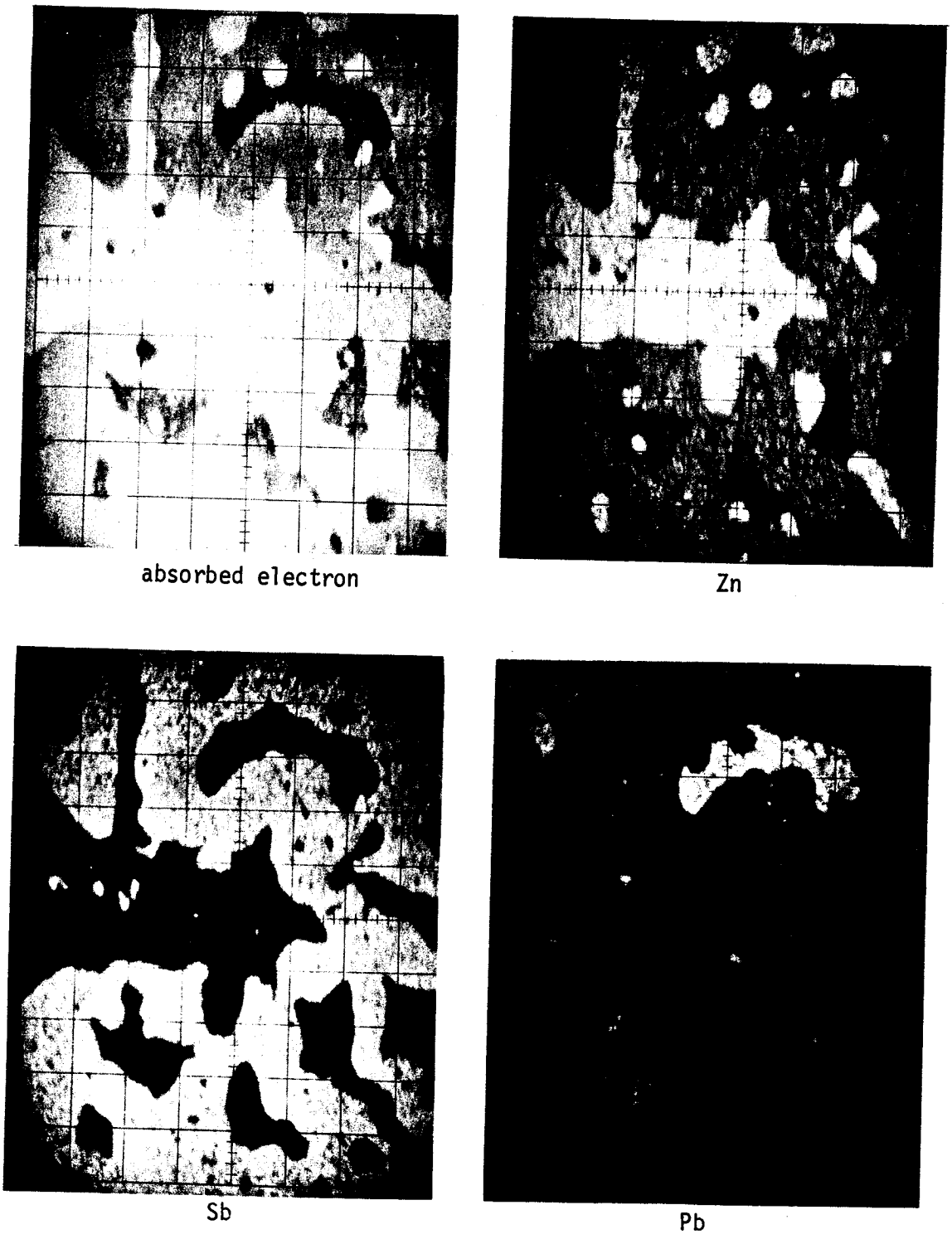

FIGURE 15. ELECTRON MICROPROBE PHOTOMICROGRAPHS OF SECTION 12B - 2 (900X)

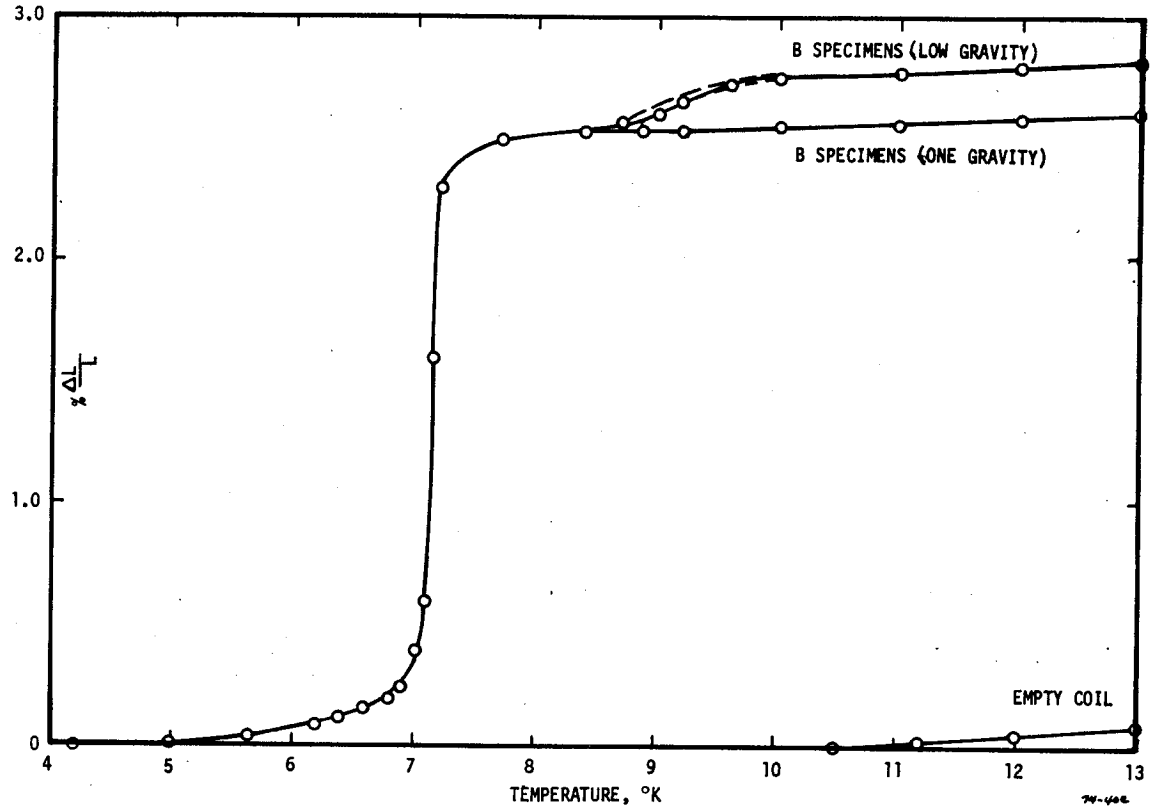

FIGURE 16. SUPERCONDUCTING TRANSITION TEMPERATURES OF B SPECIMENS

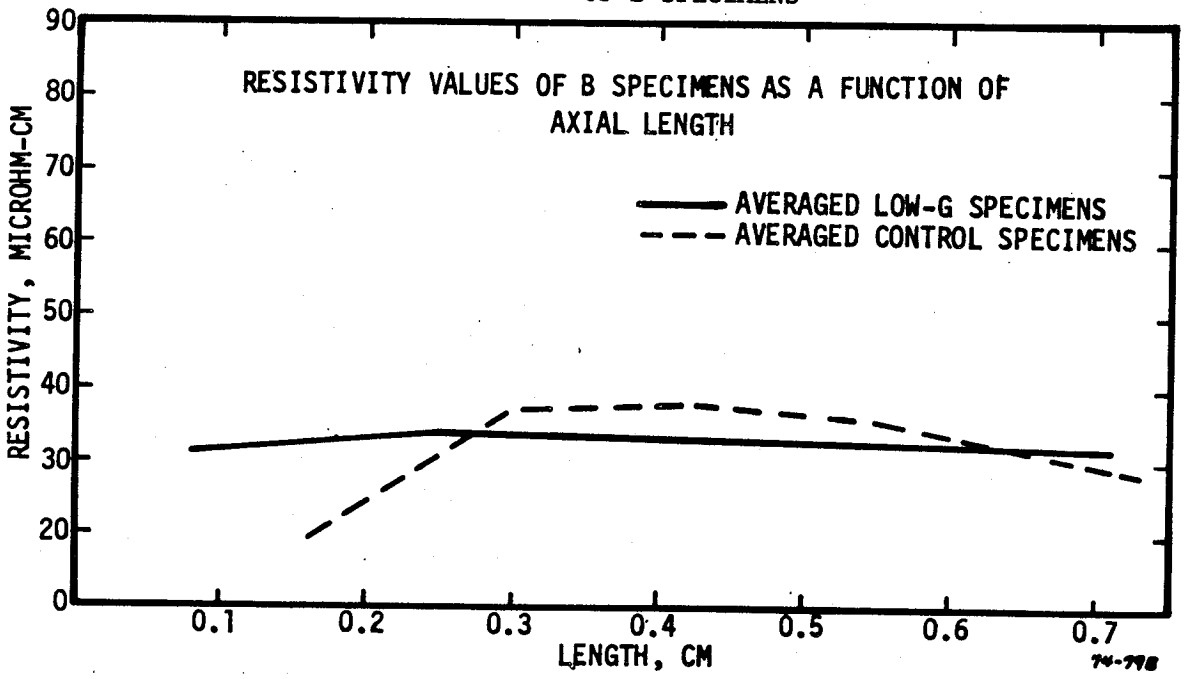

FIGURE 17. RESISTIVITY OF CONTROL AND LOW GRAVITY PROCESSED B SPECIMENS

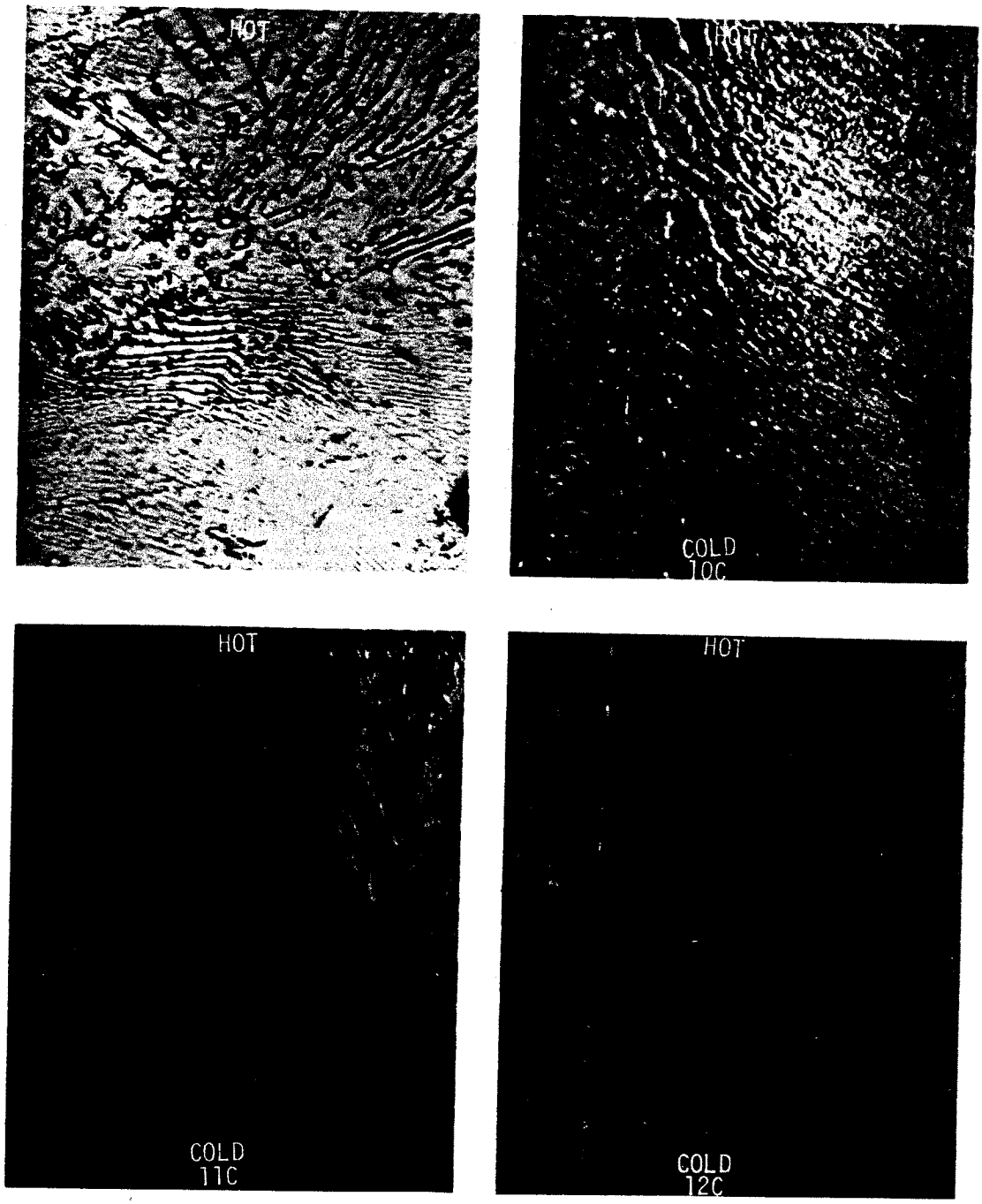

FIGURE 18. TRANSITION ZONE OF C SPECIMENS (500X)

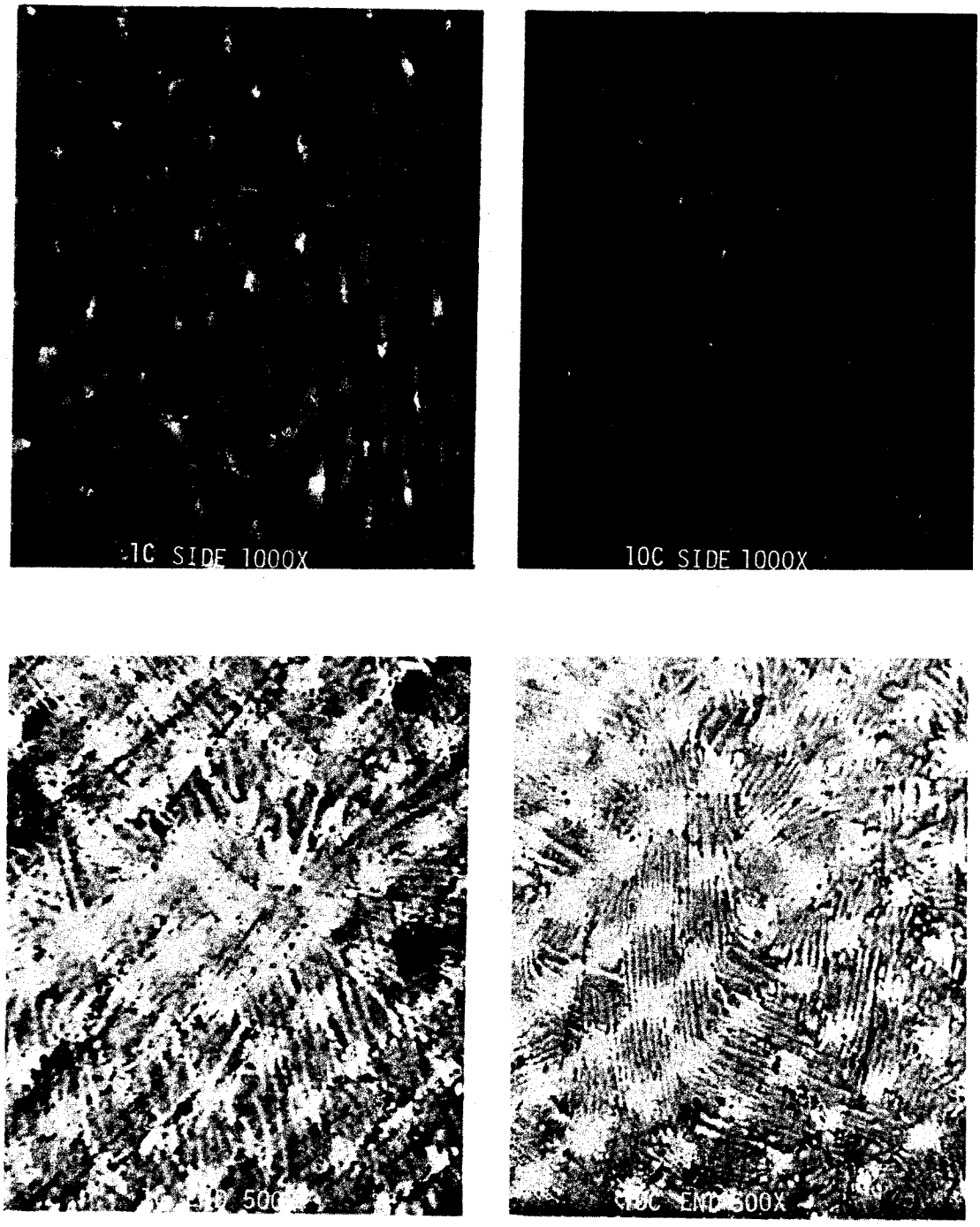

FIGURE 19. HOT ZONE PHOTOMICROGRAPHS OF C SPECIMENS

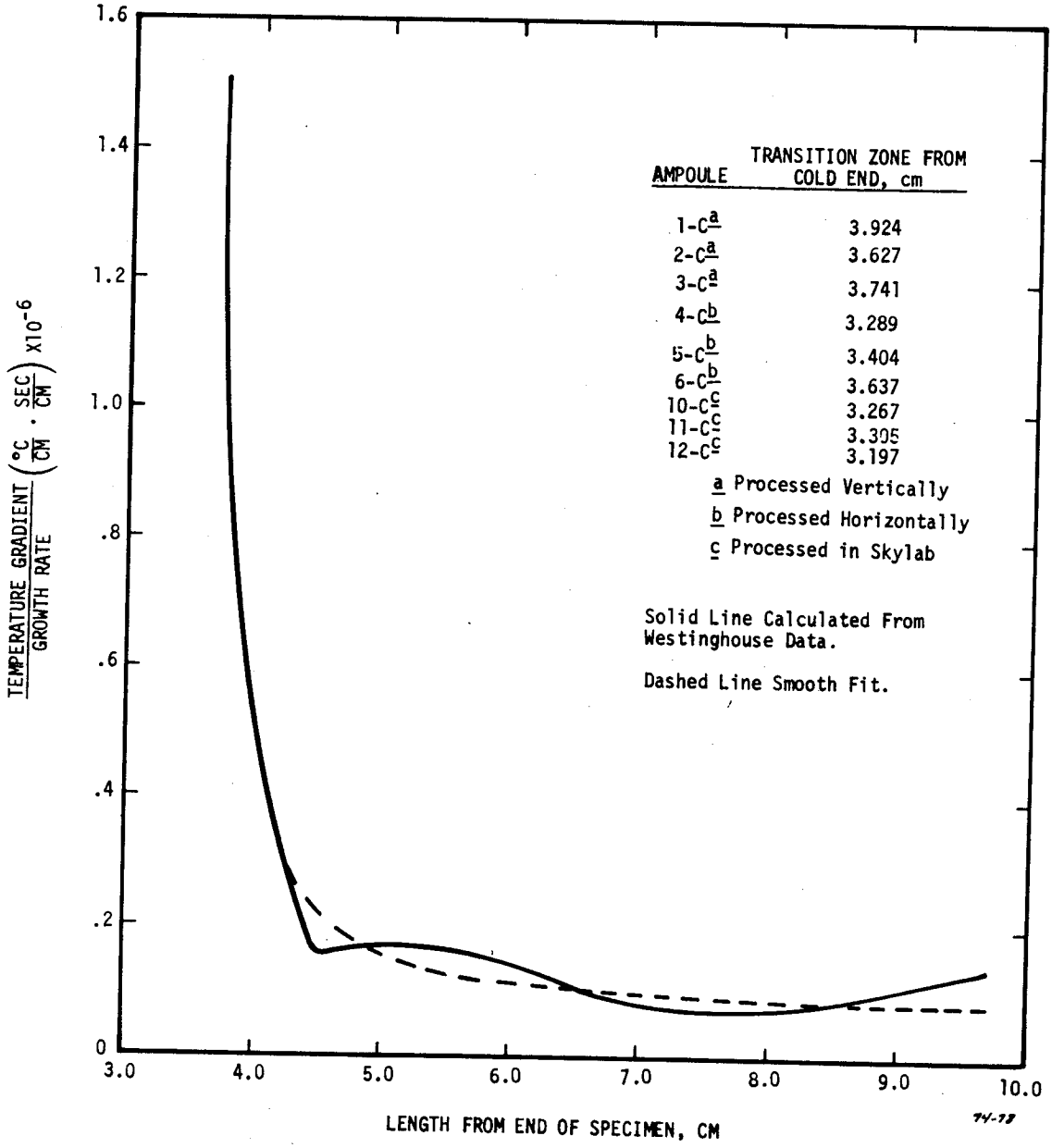

FIGURE 20. G/R RATIO AS A FUNCTION OF DISTANCE FROM COLD END

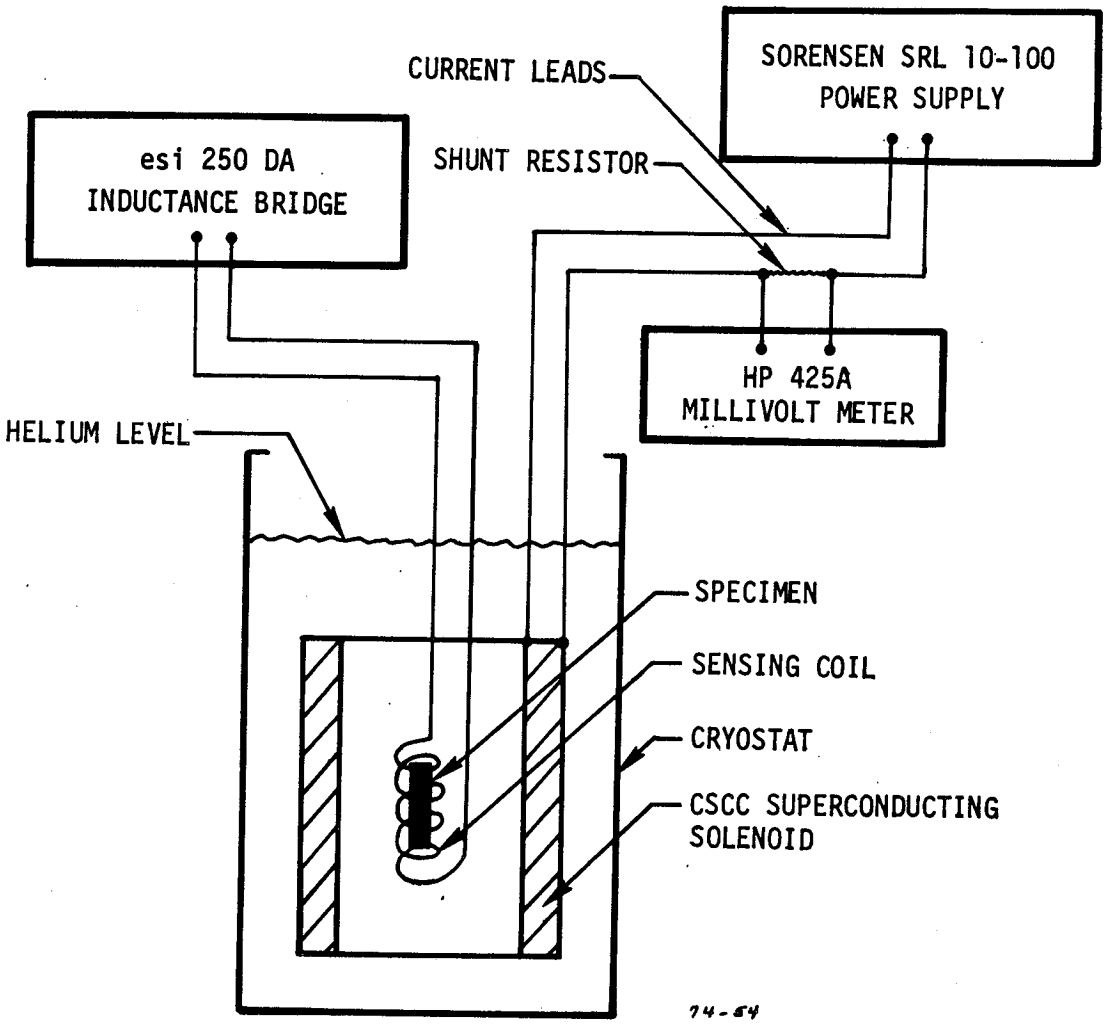

FIGURE 21. SCHEMATIC REPRESENTATION OF MAGNETIZATION MEASURING APPARATUS

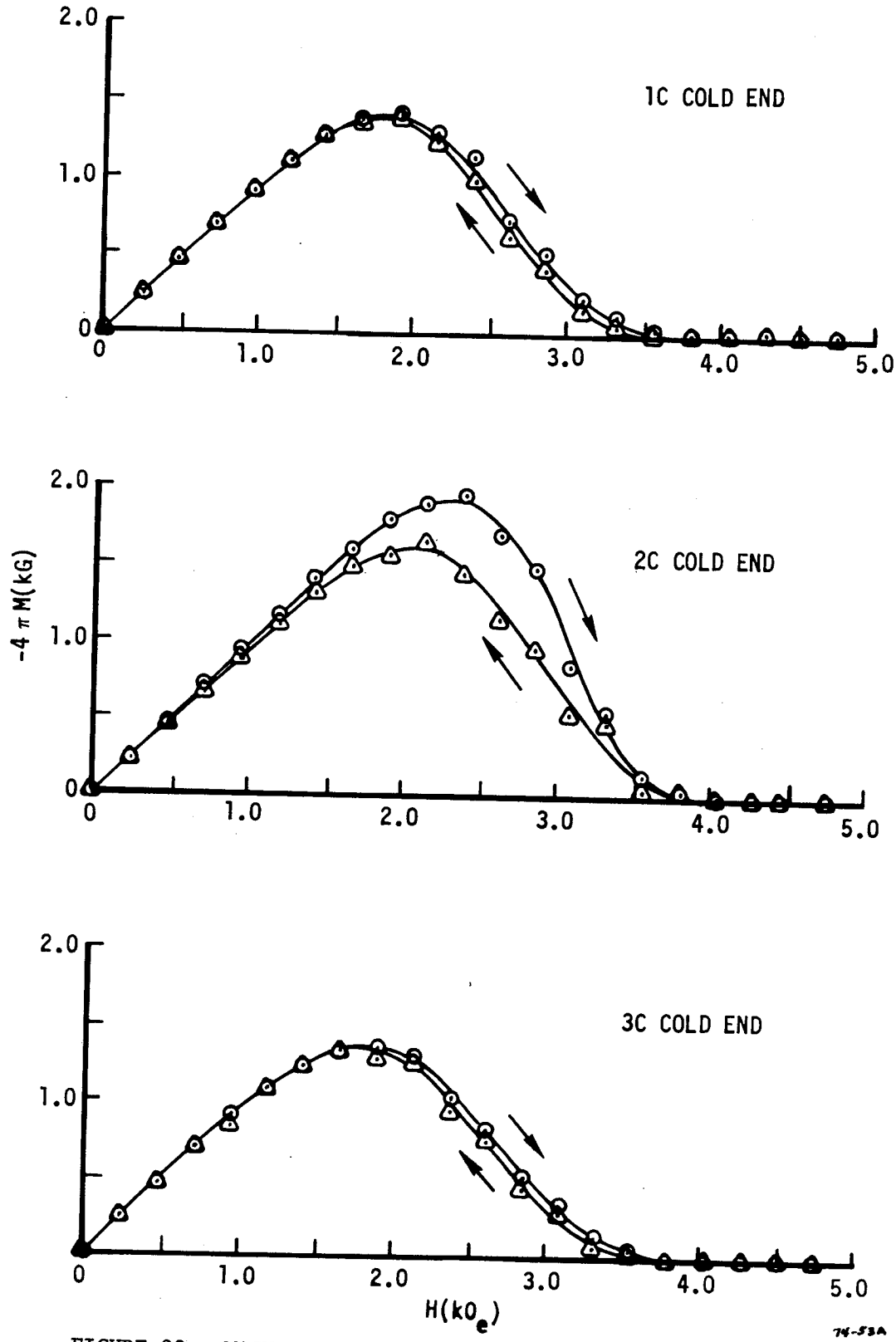

FIGURE 22. MAGNETIZATION CURVES FOR ONE GRAVITY PROCESSED C SPECIMENS

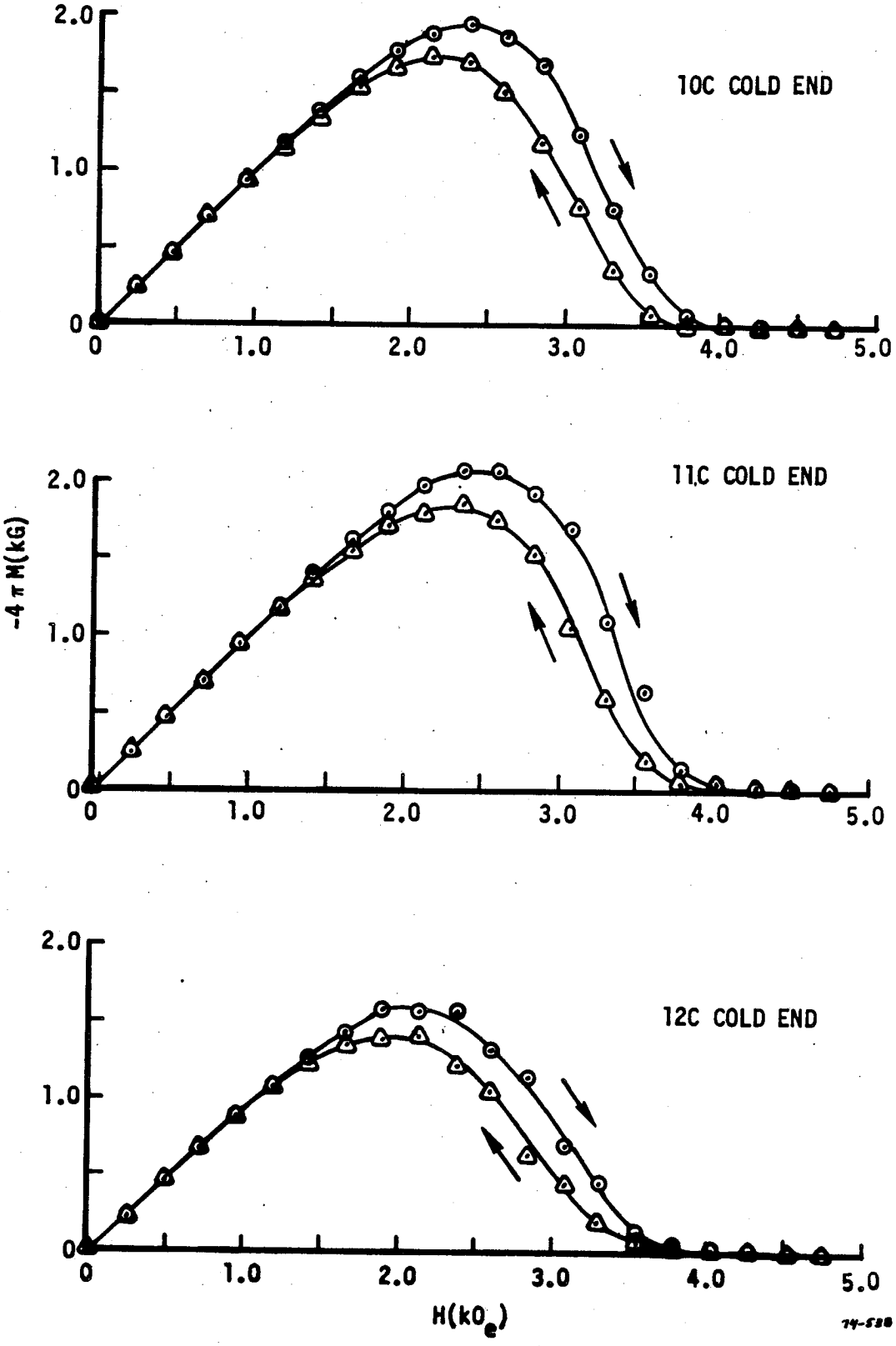

FIGURE 22. (CON'T) MAGNETIZATION CURVES FOR LOW GRAVITY PROCESSED C SPECIMENS